*Structural, Spectral, Antibacterial and Anticancer Investigations of Synthesized Isoxazole Derivatives

Elif GÜNEY [1], Koray SAYIN

Department of Chemistry, Faculty of Science, Sivas Cumhuriyet University, Sivas, TÜRKİYE

Abstract: Cancer is one of the most important diseases threatening human health today, and gastric cancer is among the top five in terms of mortality rate. Synthesized eight isoxazole derivatives were investigated in this study as computationally. Structural properties of them were examined in detail and chemical/electronic properties of these compounds are investigated using contour plot of HOMO/LUMO and molecular electrostatic potential (MEP) map. Anticancer properties of these compounds are investigated using molecular docking calculations against H. Pylori and VEGFR2. Additionally, the pharmacokinetics and pharmacology properties are investigated using ADME and p450 analyses Finally, it was found that compound 5a is the best inhibitor candidate.

Keywords: Isoxazole, Gastric Cancer, H. Pylori, VEGFR2, ADME.

1. Introduction

Gastric (stomach) cancer is the 4th place among the deadliest cancer types although it is in the 6th place in terms of incidence and initially gastric cancer occurs when cancer cells form in the lining of the stomach [1-3]. There are many risk factor of the gastric cancer which are smoking, malnutrition, and etc. *Helicobacter Pylori* (*H. Pylori*) is the one of the major risk factor for the gastric cancer. Especially it is known that *H. Pylori* infection encourages the gastric cancer in the individuals. For this reason World Health Organization (WHO) classified this bacteria as class I carcinogen. These data indicate that *H. pylori* can be selected as a target in the prevention and treatment of gastric cancer [4]. Inhibition of this bacterium is very important for human health. On the other hand, one of the other important targets is a vascular endothelial growth factor receptor 2 (VEGFR2) [5]. This target is related with vascularization and the growth of cancer cells. The inhibition of this target is one of the prevention and treatment of gastric cancer.

Isoxazole class compounds attract the attention of the researchers and drug development industry due the broad application area and easy synthesis. These compounds have many biological properties such as antiviral, antidiabetic, anticryptococcal, and anticancer [6]. Some isoxazole compounds represented in Figure 1 are used as clinically.

The aim of this study is that chemical properties of newly designed eight isoxazole derivatives are investigated by computational techniques. Biological activity of chemicals are investigated many published papers [3,7-9]. The related compounds shematic structure of them are represented in Scheme 1 are optimized at B3LYP/6-31+G(d) level in water. These compounds have been synthesized by Pallavi et al. in 2022 [6].

Spectral analyses (IR, ^{1}H-NMR and ^{13}C-NMR) are completed at same level of theory. Electronic and chemical properties are discussed using contour plots of frontier molecular orbitals, molecular electrostatic potential (MEP) map. Biological activity of these compounds against the *H. Pylori* and VEGFR2 are investigated using *in silico* techniques. For these analyses, target proteins are selected as 3MUF [10] and 6XVK [11] from protein data bank. Finally, ADME and p450 analyses of studied compounds are performed. As a results, it is found that compound 5a can be well drug candidate against *H. Pylori* and gastric cancer.

2. Computational Method
2.1. Fully Optimization

Studied compounds were fully optimized at B3LYP/6-31+G(d) level in the water phase. C-PCM method was taken into consideration to

---

[1] Corresponding Authors

e-mail: m.zakarianejad@yahoo.com & mzakarianejad@pnu.ac.ir

Elif GÜNEY, Koray SAYIN

solute-solvent interactions. In the results of calculations, no imaginary frequency was obtained. All calculations were performed in Gaussian software [12,13]. Contour plots of frontier

molecular orbitals and molecular electrostatic potential maps of studied compounds were calculated at the same level of theory.

Dicloxacillin   Cloxacillin
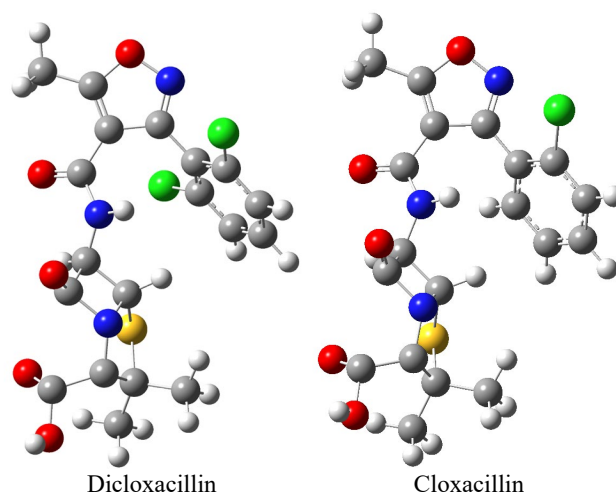
Figure 1. Geometric structure of dicloxacillin and cloxacillin
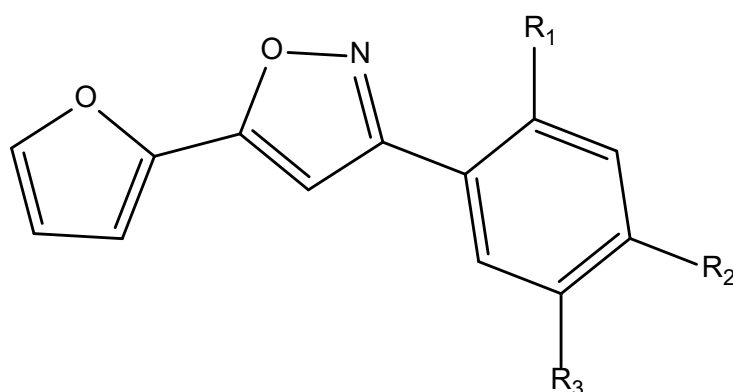
1a=R_1, R_3=H, R_2=Cl
1b=R_1, R_3=H, R_2=Br
1c=R_1, R_3=H, R_2=OCH3
1d=R_1,R_3=H, R_2=CH3
1e=R_1=OH, R_2,R_3=H
1f=R_1,R_2=Cl, R_3=H
1g=R_1,R_3=H, R_2=NO2
1h=R_1,R_3=H, R_2=F

Scheme 1. The molecular structure of studied compounds

2.2. Molecular Docking
Studied compounds were minimized at OPLS4 method at pH=7±2 using LigPrep module. On the other hand, target proteins which are 3MUF and 6XVK were minimized using Protein Preperation module. Receptor binding domain of each protein were defined using ReceptorGridGeneration module. At this stage x-y-z coordinates of 3MUF and 6XVK were selected as (26.53)-(32.42)-(-0.43) and (0.02)-(0.47)-(20.47), respectively. Molecular docking calculations were performed using Ligand Docking module. In this stage, molecular docking calculations were performed extra precision (XP). These analyses were done using Maestro 12.8 software [14-17].

2.3. ADME and p450
Pharmacokinetics and pharmacology analyses of studied compounds were done in detail.

Absorption, distribution, metabolism, and excretion (ADME) analyses were performed and some critical quantum chemical descriptors were calculated. These calculations were done using "Ligand-Based ADME/Tox Prediction" module. Furthermore, p450 analyses of studied compounds were performed. All calculations in this analysis are performed against CYP2C9 using "p450 site of metabolism" module.

3. Results and discussion
3.1. Optimized Structures
The studied isoxazole derivatives are optimized at B3LYP/6-31+G(d) level in water. Optimized structures with atomic labelings of studied compounds are represented in Figure 1. The geometric parameters which are the bond lengths (Å), bond angles (degrees) and dihedral angles (degrees) of them are given in Table 1.

According to Fig. 1 and dihedral angles, the planar structure is dominant for the studied compounds and geometric parameters are similar to each other. Furthermore, calculated geometric parameters are compared with data in literature. In published articles, the bond lengths of C-C, C-O, C-N are reported in the range of 1.399 – 1.421 cm⁻¹, 1.313 – 1.356 cm⁻¹ and 1.331 – 1.449 cm⁻¹, respectively [18-21]. These experimental values are showed that calculated geometric parameters are in good agreement with the published data.

Table 1. Geometric parameters of compounds calculated at B3LYP/6-31+G (d) level

Assignments	1a	2a	3a	4a	5a	6a	7a	8a
Bond Lengths (Å)								
C1-C2	1.428	1.428	1.429	1.429	1.429	1.428	1.428	1.428
C3-O1	1.361	1.360	1.361	1.361	1.361	1.361	1.360	1.361
C4-C5	1.441	1.440	1.441	1.441	1.441	1.440	1.440	1.441
C5-O2	1.352	1.352	1.352	1.352	1.352	1.353	1.353	1.352
O2-N1	1.394	1.395	1.398	1.397	1.399	1.393	1.390	1.395
N1-C7	1.323	1.323	1.323	1.323	1.321	1.323	1.323	1.322
C7-C8	1.474	1.473	1.471	1.474	1.475	1.476	1.474	1.474
C8-C9	1.405	1.405	1.402	1.404	1.410	1.407	1.407	1.407
Bond Angle (deg.)								
C1-C2-C3	106.1	106.1	106.1	106.1	106.1	106.1	106.1	106.1
C3-O1-C4	107.1	107.0	107.1	107.1	107.1	107.0	107.0	107.1
C4-C5-C6	132.1	132.1	132.0	132.0	132.1	132.0	132.2	132.1
C4-C5-O2	118.3	118.3	118.3	118.3	118.4	118.4	118.3	118.3
C5-O2-N1	109.1	109.1	109.1	109.1	109.4	109.2	109.3	109.1
C5-C6-C7	104.1	104.1	104.2	104.2	104.1	103.9	104.0	104.1
C7-C8-C9	120.6	120.6	120.9	120.8	122.8	118.4	120.4	120.5
C9-C10-C11	119.3	119.3	119.7	121.4	120.6	118.8	120.6	118.6
Dihedral Angle (deg.)								
C1-C2-C3-O1	0.0	0.0	0.0	-0.0	-0.0	-0.0	0.0	-0.0
C2-C3-O1-C4	-0.0	-0.0	-0.0	0.0	-0.0	0.0	-0.0	0.0
C4-C5-C6-C7	179.9	179.9	179.9.	-179.9	-179.4	-179.9	-179.9	179.9
C4-C5-O2-N1	-179.9	-179.9	-179.9	179.9	179.5	179.9	179.9	-179.9
C5-O2-N1-C7	0.0	0.0	0.1	0.0	-0.0	0.0	0.0	0.0
O2-N1-C7-C8	179.9	179.9	179.4	-179.9	178.5	-176.8	-179.9	179.9
N1-C7-C8-C9	-1.0	-0.0	-11.6	2.2	40.2	36.6	1.4	-0.8
C9-C10-C11-C12	-0.0	-0.0	-0.0	0.0	-0.2	0.5	0.0	-0.0

3.2. Simulated IR Spectra

Infrared spectroscopy (IR spectroscopy or vibrational spectroscopy) is the measurement of the interaction of infrared radiation with matter through absorption, emission or reflection. It is used to study and identify solid, liquid or gaseous chemical substances or functional groups. It is mainly used to characterize new materials or to identify and validate known and unknown samples. IR spectrum can be obtained both experimentally and computationally. In this study, IR spectrum of studied compounds are calculated and represented in Figure 2.

According to Table 2, aromatic CH stretching frequency is calculated nearly 3200 cm⁻¹ while this frequency has been reported in the range of 3105 – 3001 cm⁻¹ [22]. In aliphatic CH stretching frequency, it is calculated in the range of 3036 – 3157 while it has been reported in the range of 3050 – 2850 [9]. For our studied compounds, stretching frequency of C=N bond is calculated in the range of 1461 – 1531 cm⁻¹ [23] As for the other peaks, the stretching frequencies of CO and CN are calculated nearly 1310 and 960 cm⁻¹, respectively. These frequencies, CO and CN, have been reported in the range of 1334 - 1417 and 925 – 970, respectively [23, 24].

3.3. Simulated NMR Spectra

Nuclear magnetic resonance spectroscopy, commonly known as NMR spectroscopy, is a research technique that uses certain magnetic properties of atomic nuclei. ^{1}H-NMR and ^{13}C-NMR of studied compounds are calculated and chemical shift values of hydrogen and carbon atoms are given in Table 3 respecto to tetramethylsilane (TMS).
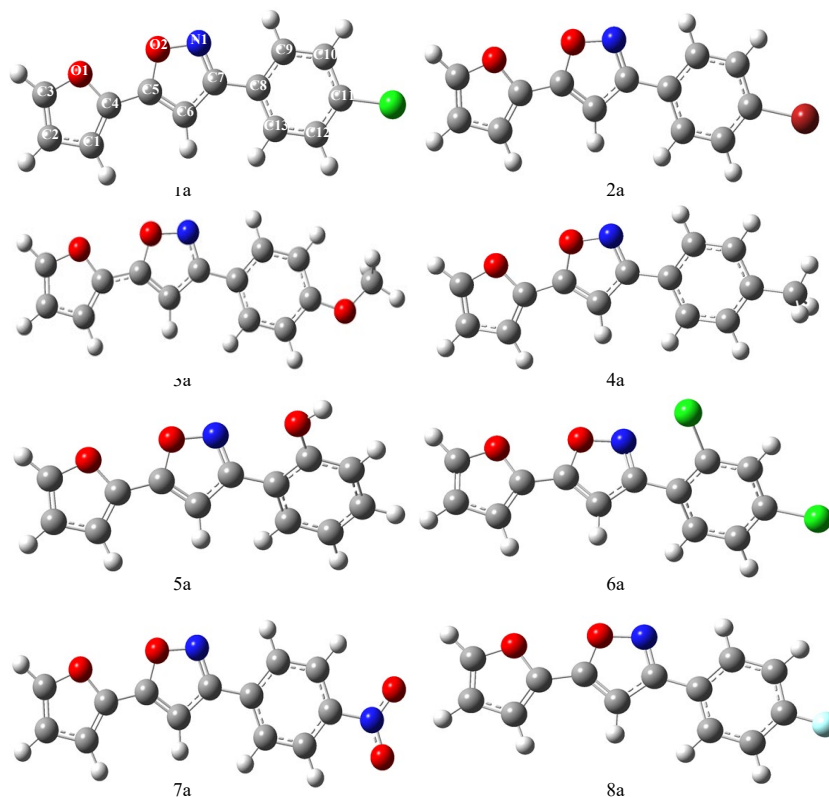
Figure 2. Optimized structure of investigated compounds.
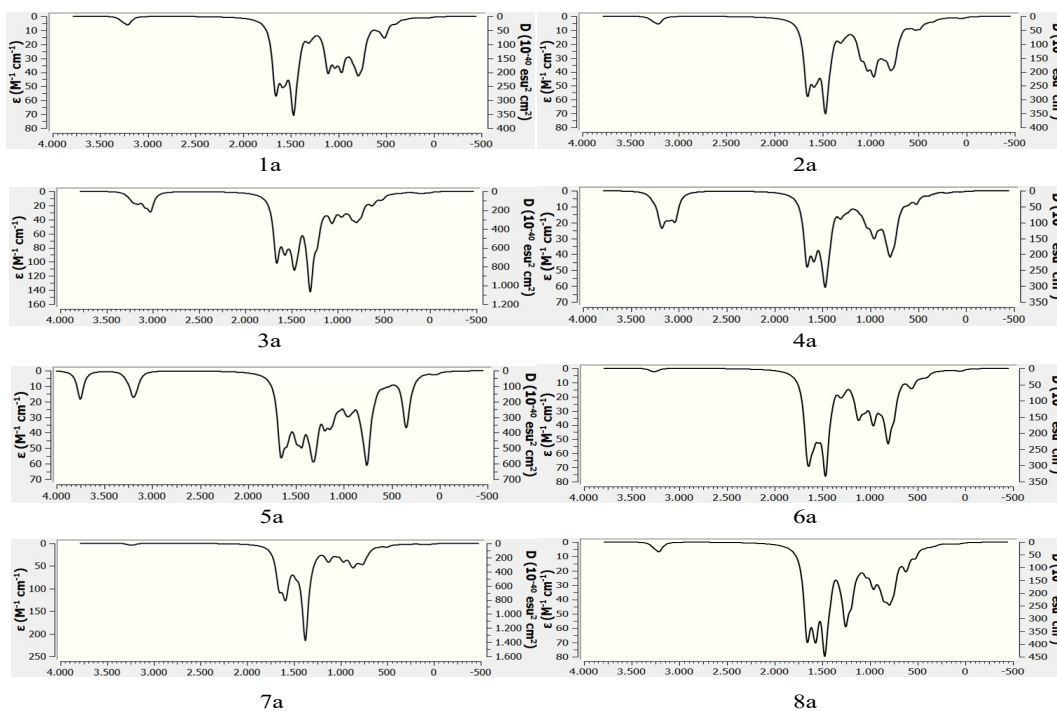
Figure 3. The calculated IR spectrums of studied compounds.

Table 2. Vibrational frequencies (cm^{-1}) of some functional groups in studied compounds

Assignment	1a	2a	3a	4a	5a	6a	7a	8a
$\nu_{CH aromatic}$	3211	3222	3213	3177	3195	3263	3225	3213
$\nu_{CH aliphatic}$	-	-	3157	3036	-	-	-	-
ν_{CC}	1662	1649	1661	1668	1662	1638	1663	1663
$\nu_{C=N}$	1482	1483	1487	1483	1531	1461	1484	1485
ν_{CO}	1310	1311	1311	1311	1310	1311	1309	1311
ν_{NO}	961	960	950	955	938	959	968	959

Table 3 Spectral data for compounds calculated at level B3LYP/6-31+G (d)

Assignments	1a	2a	3a	4a	5a	6a	7a	8a
^{13}C-NMR								
C1	105.9	106.0	105.1	105.2	105.1	106.2	106.8	105.7
C2	107.2	107.1	107.1	107.0	107.0	107.4	107.4	107.1
C3	139.1	139.1	138.5	138.7	138.4	139.0	139.8	139.0
C4	140.2	140.1	140.8	140.7	140.8	140.2	139.7	140.3
C5	157.8	157.8	157.2	157.3	156.5	157.2	158.5	157.7
C6	90.3	90.4	90.7	90.5	94.5	95.6	90.7	90.5
C7	155.6	155.8	156.9	156.4	156.8	156.8	155.3	155.8
C8	124.1	124.7	118.6	123.3	114.8	124.4	132.4	122.5
C9	122.7	122.7	123.8	122.1	150.0	127.5	122.2	124.2
C10	124.9	128.1	104.8	125.1	110.3	122.6	121.3	112.4
C11	140.0	137.8	155.4	135.3	124.7	139.8	143.9	160.5
C12	123.5	126.8	113.3	123.3	115.0	125.6	120.6	111.0
C13	122.1	122.2	123.2	121.7	127.1	137.7	121.4	123.1
^{1}H-NMR								
C1*H*	6.6	6.6	6.6	6.6	6.6	6.7	6.7	6.6
C2*H*	6.4	6.4	6.4	6.4	6.4	6.4	6.4	6.4
C3*H*	7.5	7.5	7.4	7.5	7.4	7.5	7.5	7.5
C6*H*	6.3	6.3	6.4	6.3	6.1	6.5	6.3	6.3
C9*H*	8.3	8.3	8.3	8.3	7.2	7.8	8.5	8.4
C10*H*	7.3	7.4	6.5	7.2	6.4	7.1	8.3	7.1
C12*H*	7.2	7.4	6.9	7.2	6.9	7.3	8.3	7.0
C13*H*	7.3	7.3	7.4	7.4	7.3	7.3	7.5	7.4

3.4. Electronic Properties

Electronic properties of compounds provision essential clues about chemical properties of compounds. There are a lot of way to learn these properties which are molecular electrostatic potential (MEP) map, MEP contour and contour plot of molecular orbitals. Some of them are calculated and given at below.

3.4.1. Contour plot of HOMO and LUMO

Contour plot of the highest occupied molecular orbital (HOMO) and the lowest unoccupied molecular orbital (LUMO) are calculated at same level of theory and represented in Figure 3.

HOMO and LUMO are the most well-known chemical parameters. These orbitals are known as frontier molecular orbitals. HOMO indicates an electron donating ability while LUMO implies the electron accepting ability. According to Fig. 3, there are two colors, red and green, in the contour plots of the frontier molecular orbitals. It can be said that pi electrons on the benzene ring are generally delocalized on the whole structure and the pi electrons increase the reactivity of the molecules.

Elif GÜNEY, Koray SAYIN

Both HOMO and LUMO, these compounds can be interacted with their pi electrons easily.

3.4.2. MEP Maps

Molecular electrostatic potential (MEP) maps are a common diagram to describe reactive site of the compounds. MEP maps are useful in the determination of the nucleophilic and electrophilic active sites. Additionally, every shape, shape size and color in the MEP map has a meaning. These illustrations imply the reactivity of the compounds. MEP map of studied compounds are calculated at same level of theory and represented in Figure 4.
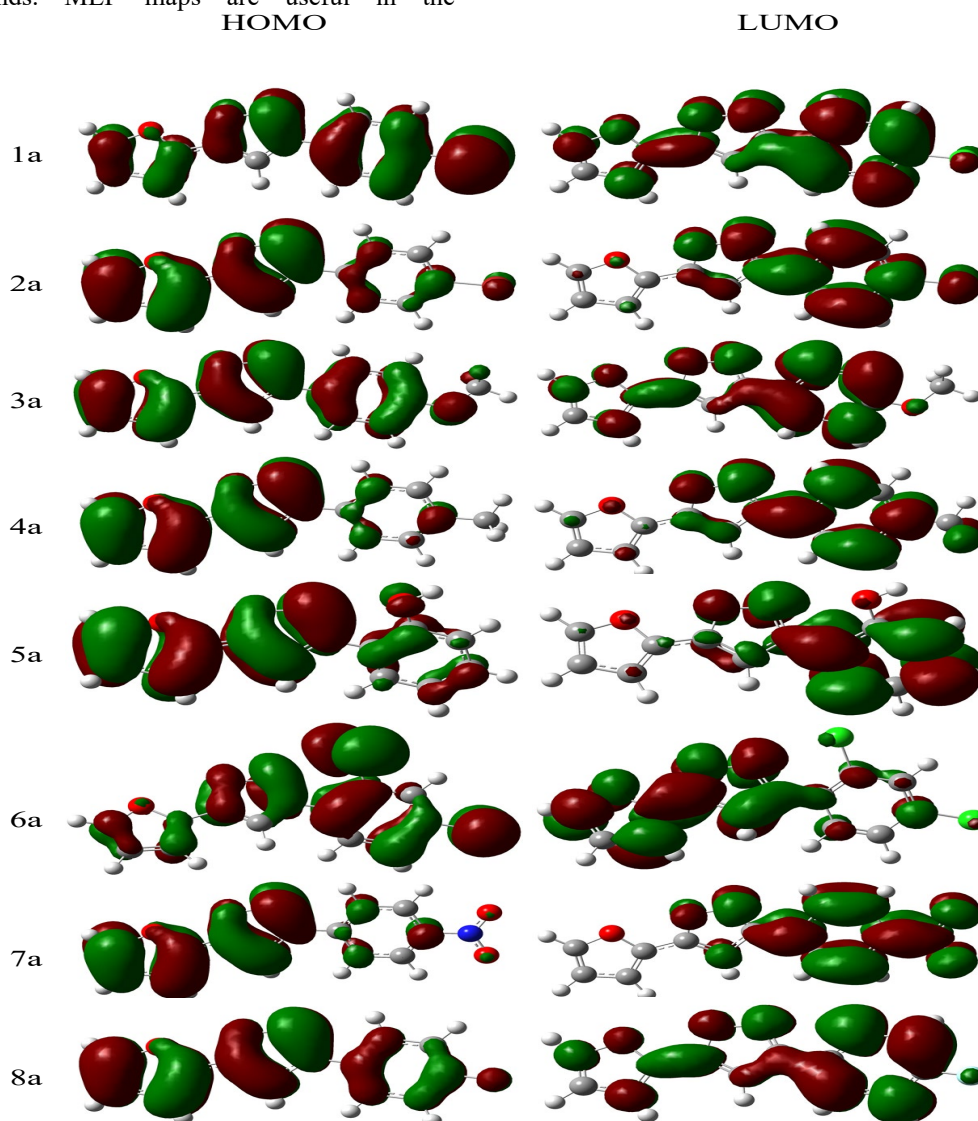
Fig. 4. Contour diagram of frontier molecular orbitals.
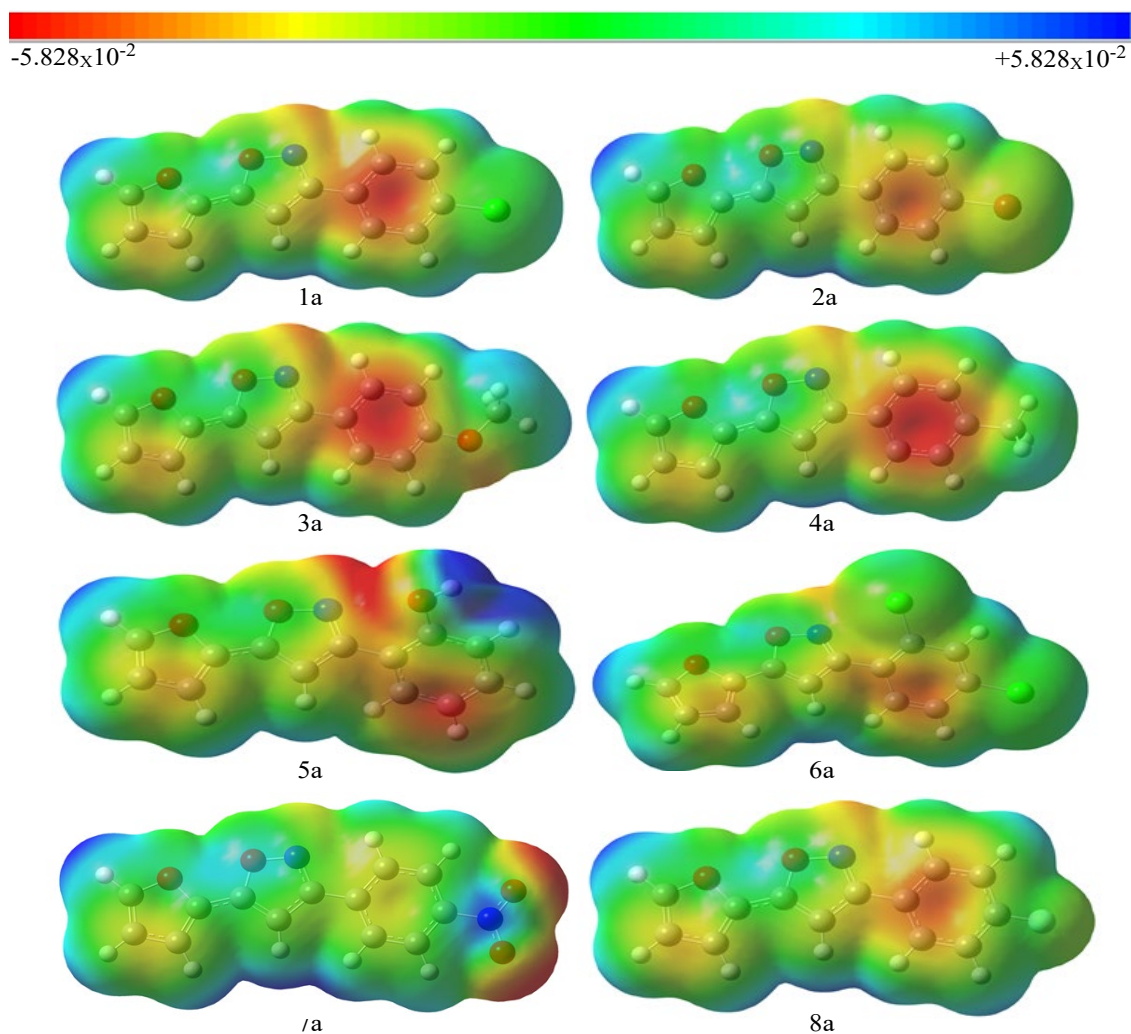
Fig. 5. Molecular electrostatic potential maps for studied compounds.

Table 4. Molecular docking results

Compounds	DS[a]	E_{vdW}[a]	E_{Coul}[a]	E_{Total}[a]
3MUF				
1a	-4.011	-28.445	-0.670	-29.114
2a	-3.953	-30.664	-1.862	-32.525
3a	-4.446	-27.794	-3.714	-31.508
4a	-3.602	-29.547	0.616	-28.931
5a	-5.576	-26.605	-4.435	-31.040
6a	-3.747	-32.359	-0.860	-33.219
7a	-3.756	-32.068	-0.278	-32.346
8a	-4.526	-27.917	-0.590	-28.507
6VXK				
1a	-7.416	-34.544	-1.047	-35.591
2a	-8.016	-31.409	0.831	-30.578
3a	-7.517	-29.741	-1.172	-30.913
4a	-7.572	-31.504	-0.911	-32.415
5a	-10.249	-32.436	-5.867	-38.303
6a	-7.741	-36.469	0.460	-36.009
7a	-7.187	-34.834	-0.128	-34.962
8a	-7.691	-28.008	0.858	-27.150

[a] in kcal/mol

Fig. 6. The complex structures and interaction map between compound 5a and target proteins (3MUF and 6VXK).

According to Fig. 4, pi electrons still appear to be active. Additionally, environment of the heteroatoms are generally red and it means that these sites are appropriate fort he electrophilic attack. As a result, there are many active site on the molecular surface and these compounds can be easily interact with the appropriate sites.

3.5. Molecular Docking

Affinity of our compounds against *H. Pylori* and VEGFR2 are investigated via molecular docking calculations. Interactions between inhibitor candidate and target proteins are examined. Molecular docking analyses are performed and docking score (DS), van der Waals interaction energy (E_{vdW}), Coulomb interaction energy (E_{Coul}) and total interaction energy (E_{Total}) are given in Table 4.

According to Table 4, it seems that compound 5a is the best inhibitor candidate due to the fact that this compound exhibits the best inhibition properties against the target protein. Generally, electrostatic interactions are so weak, that even for some ligands this value appears to be positive. However, van der Waals interactions are good between inhibitor candidates and target proteins. As for the total interactions, this value is similar to each other. Among all the results, the most important parameter is the docking score. The docking score is a measure of the key-lock harmony between the inhibitor candidate and the protein. *H. Pylori* and VEGFR2 are among the most important targets for gastric cancer. For that reason, the inhibitor candidate, which is effective for both targets, is expected to be effective in gastric cancer as well. The complex structure and interaction map between compound 5a and target proteins is represented in Figure 5.

Elif GÜNEY, Koray SAYIN

According to Fig. 5, there are restricted electrostatic interactions and hydrophobic, polar and glycine interactions are dominant in each complex structure. Additionally, H-bond, pi-cation and pi-pi stacking interactions are observed. Finally, it can be said that the interaction between compound 5a and 6VXK is so good.

3.6. ADME and p450 Analyses
Pharmacokinetics and pharmacology analyses of studied compounds are completed by ADME and p450 calculations. For ADME analyses, many molecular descriptors are calculated and compared to the reference data. Calculated descriptors are given in Table 5.

According to Table 5, calculated parameters are in the good agreement with the recommended value for each parameters. These parameters reveal the druglikeness properties of the investigated compounds. Especially, these compounds have skin permeability, MDCK cell permeability, Caco-2 cell permeability, brain/blood permeability. Additionally, some compounds can be taken part in metabolic reactions which it is undesirable. In such cases, the dose of the drugs taken into the body should be adjusted. p450 metabolism analyzes are required for a clearer prediction and the affinities of the compounds against CYP2C9 enzymes are investigated for only compound 5a. The p450 cytochrome analysis of this compound are represented in Figure 6.

Table 5. Calculated QikProp parameters of studied boron compounds for ADME analyses

Parameters[a]	1a	2a	3a	4a	5a	6a	7a	8a	RV[b]
Stars	0	0	0	0	0	0	0	0	0-5
Amine	0	0	0	0	0	0	0	0	0-1
SASA	469.8	474.8	481.8	478.1	454.6	487.0	486.9	454.7	300.0-1000.0
FOSA	0	0	93.30	88.21	0	0	0	0	0.0-750.0
FISA	42.27	42.24	42.21	42.21	79.63	34.72	139.94	42.27	7.0-330.0
PISA	355.99	355.24	346.26	347.67	374.99	322.60	346.93	365.59	0.0-450.0
WPSA	71.54	77.28	0	0	0	129.68	0	46.84	0.0-175.0
DonorHB	0	0	0	0	1	0	0	0	0.0-6.0
AccptHB	2.00	2.00	2.75	2.00	2.75	2.00	3.00	2.00	2.0-20.0
QPpolrz	27.76	28.10	28.29	28.32	26.28	28.90	28.28	26.72	13.0-70.0
QPPCaco	3935.52	3938.68	3941.48	3941.44	1740.94	4641.70	466.49	3935.54	<25 poor >500 great
QPlogBB	0.36	0.37	0.12	0.18	-0.20	0.56	-0.78	0.30	-3.0- 1.2
QPPMDCK	5362.38	5770.50	2178.65	2178.62	900.76	10000.00	216.98	3927.03	<25 poor >500 great
QPlogKp	-1.04	-1.05	-0.98	-1.07	-1.57	-1.02	-2.78	-1.01	-8.0- -1.0
metab	1	1	2	2	2	1	2	1	1-8
QPlogKhsa	0.30	0.32	0.15	0.34	0.06	0.40	0.08	0.22	-1.5- 1.5
Percent Human-Oral Absorption	100.00	100.00	100.00	100.00	100.00	100.00	89.06	100.00	>80% is high <25% is poor
PSA	33.73	33.73	41.92	33.72	52.85	32.13	78.75	33.73	7.0- 200.0
RuleOfFive	0	0	0	0	0	0	0	0	Max is 4
RuleOfThree	0	0	0	0	0	0	0	0	Max is 3

[a] **Stars**: Number of property or descriptor values that fall outside the 95% range of similar values for known drugs; **Amine**: Number of non-conjugated amine groups; **rtvFG**: Number of reactive functional groups; **SASA**: Total solvent accessible surface area; FOSA: Hydrophobic component of the SASA; **FISA**: Hydrophilic component of the SASA; **PISA**: π (carbon and attached hydrogen) component of the SASA; **WPSA**: Weakly polar component of the SASA; **donorHB**: Estimated number of hydrogen bonds that would be donated; **AccptHB**: Estimated number of hydrogen bonds that would be accepted; **QPpolrz**: Predicted polarizability in cubic angstroms; **QPPCaco**: Predicted apparent Caco-2 cell permeability in nm/sec; **QPlogBB**: Predicted brain/blood partition coefficient; **QPPMDCK**: Predicted apparent MDCK cell permeability in nm/sec; **QPlogKp**: Predicted skin permeability; **metab**: Number of likely metabolic reactions; **QPlogKhsa**: Prediction of binding to human serum albumin; **PercentHuman-OralAbsorption**: Predicted human oral absorption on 0 to 100% scale; **PSA**: Van der Waals surface area of polar nitrogen and oxygen atoms; **RuleOfFive**: Number of violations of Lipinski's rule of five; **RuleOfThree**: Number of violations of Jorgensen's rule of three.
[b] RV: Recommended Value

Fe-Accessibility   Instrinsic Reactivity   Overall SOM Score   Combined
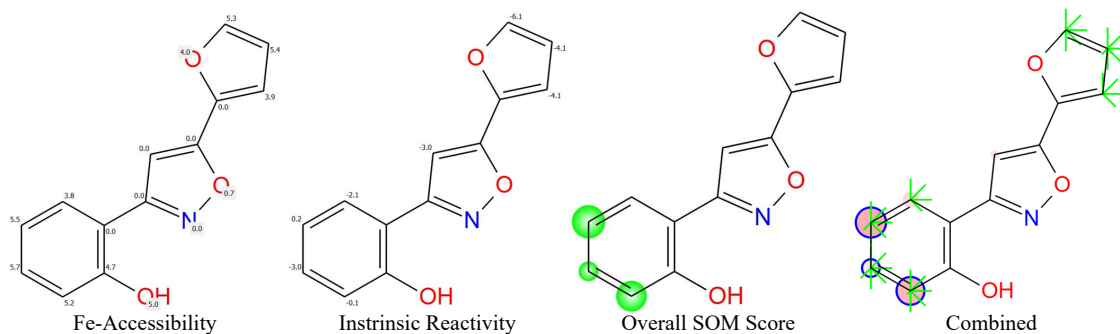
Fig. 7. p450 cytochrome analysis of compound 5a.
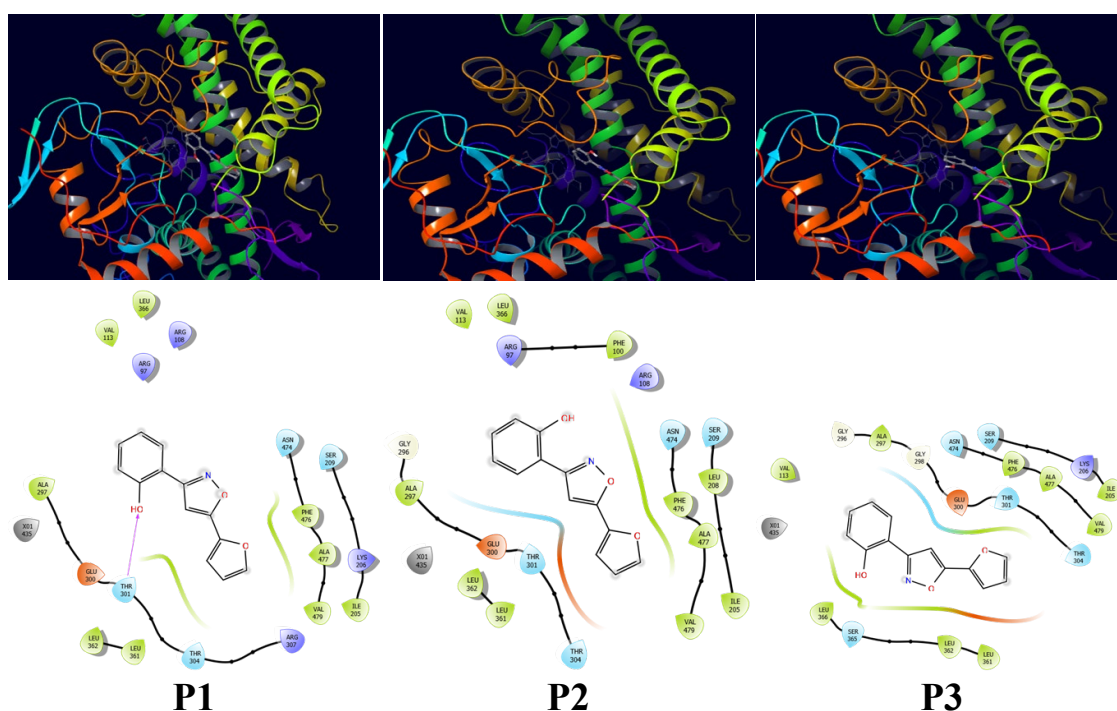
Fig. 8. Complex structure between 5a and CYP2C9.

Table 6. p450 cytochrome analysis of 5a against CYP2C9

Pose	DS[a]	E_{vdW}[a]	E_{Coul}[a]	E_{Total}[a]
1	-6.557	-32.104	-1.107	-33.211
2	-6.753	-33.727	-1.143	-34.870
3	-6.754	-31.912	-1.202	-33.114

[a] in kcal/mol

According to Fig. 6, some atoms in compound 5a have instrinsic reactive. So, compound 5a seems so reactive. As for the iron accessibility, total seven atoms can interact with the Fe atom in the CYP enzyme. Furthermore, it is calculated that compound 5a inhibited the CYP2C9 enyzme. There are total three different poses for compound 5a and the complex structure belong these poses are represented in Figure 7. Furthermore, the docking results between 5a and CYP2C9 are given in Table 6.

According to Fig. 7 and Table 6, CYP2C9 enzyme is inhibited by compound 5a. Actually, this situation is undesirable.

When the drug in question is taken into the body, it indicates that drug accumulation will occur. For that reason, dose adjustments of both this drug and, if taken, other drugs should be made when this drug is taken into the body.

4. Conclusions

Isoxazole derivatives are optimized at B3LYP/6-31+G(d) level in water. Structural and electronic properties of studied compounds are examined in detail. Especially, spectral characterization of studied compounds are performed using IR and 1H-NMR and 13C-NMR. Electronic and chemical properties of these compounds are examined using contour plot of frontier molecular orbital and molecular electrostatic potential maps. Additionally, anticancer properties of studied compounds against H. Pylori and VEGFR2 are investigated in detail. Compound 5a is found as the most active compound and pharmacokinetics and pharmacology analyses of it are done using ADME and p450 analyses. It is found that CYP2C9 enzyme is inhibited by 5a and drug dose adjustment should be done in further analyses.

Author contribution EG performed the computational studies. KS designed the experiments and consistent guidance; analyzed the data, manuscript preparation, and review; edited the fnal version; and submitted it for publication.

Availability of data and material All experimental data were included in the article.

Competing interests The authors declare no competing interests.

References

[1] C. de Martel, D. Georges, F. Bray, J. Ferlay, G.M. Clifford, Global burden of cancer attributable to infections in 2018: a worldwide incidence analysis, Lancet glob. Health 8(2020):e180-e190.

[2] https://www.who.int/news-room/fact-sheets/detail/cancer (Access Date: 24.05.2022)

[3] M. Gömeç, Z. Hasbek, Investigation of 18F-FDG Pet/Ct and Clinicopathological Data Of Diffuse Type Gastric Cancers, Kırıkkale Üniversitesi Tıp Fakültesi Dergisi 24 (2022) 102-109.

[4] J. Parsonnet *Helicobacter Pylori* and Gastric Cancer. Gastroenterology Clinics of North America 22 (1993) 89-104.

[5] G. Roviello, K. Polom, F. Roviello, D. Marrelli, A. G. Multari, G. Paganini, C. Pacifico, D. Generali, Targeting VEGFR-2 in Metastatic Gastric Cancer: Results From a Literature-Based Meta-Analysis. Cancer Investigation 35 (2017) 187-194.

[6] P. HM, F. H. Al-Ostoot, H.K. Vivek, S. A. Khanum, Synthesis, characterization, DFT, docking studies and molecular dynamics of some 3-phenyl-5-furan isoxazole derivatives as anti-inflammatory and anti-ulcer agents. Journal of Molecular Structure 1250 (2022) 131812.

[7] S. Akkoç, B. Tüzün, A. Özalp, Z. Kökbudak, Investigation of structural, electronical and in vitro cytotoxic activity properties of some heterocyclic compounds. J. Mol. Struct. 1246 (2021) 131127.

[8] A. Aktaş, B. Tuzun, A.H. Taskin, K. Sayin, H. Ataseven, How do arbidol and its analogs inhibit the SARS-CoV-2?. Bratislava Med. J. 121 (2020) 705-711.

[9] M.A. Gedikli, B. Tuzun, A. Aktas, K. Sayin, H. Ataseven, Are clarithromycin, azithromycin and their analog effective in the treatment of COVID19?. Bratislava Med. J. 122 (2021) 101–110.

[10] W.C. Cheng, YF. Chen, HJ. Wang, KC. Cheng Hsu, SC. Lin, TJ Chen, JM. Yang, WC. Wang, Shikimate kinase from Helicobacter pylori in complex with shikimate-3-phosphate and ADP. PloS One 7 (2012) e33481-e33481.

[11] M. Schimpl, K. McAuley, E.A. Hoyt, M. Thomas, M.S. Bodnarchuk, H. J. Lewis, D. Barratt, M. J. Deery, D. J. Ogg, G. J. L. Bernardes, R. A. Ward, J. G. Kettlei M. J. Waring, Crystal structure of the KDR

(VEGFR2) kinase domain in complex with a type-II inhibitor bearing an acrylamide, J Am Soc 142 (2020) 10358-10372.

[12] Roy Dennington, Todd A. Keith, John M. Millam, GaussView, Version 6.1, Semichem Inc., Shawnee Mission. KS,. (2016).

[13] M. J. Frisch, G. W. Trucks, H. B. Schlegel, G. E. Scuseria, M. A. Robb, J. R. Cheeseman, G. Scalmani, V. Barone, G. A. Petersson, H. Nakatsuji, X. Li, M. Caricato, A. V. Marenich, J. Bloino, B. G. Janesko, R. Gomperts, B. Mennucci, H. P. Hratchian, J. V. Ortiz, A. F. Izmaylov, J. L. Sonnenberg, D. Williams-Young, F. Ding, F. Lipparini, F. Egidi, J. Goings, B. Peng, A. Petrone, T. Henderson, D. Ranasinghe, V. G. Zakrzewski, J. Gao, N. Rega, G. Zheng, W. Liang, M. Hada, M. Ehara, K. Toyota, R. Fukuda, J. Hasegawa, M. Ishida, T. Nakajima, Y. Honda, O. Kitao, H. Nakai, T. Vreven, K. Throssell, J. J. A. Montgomery, J. E. Peralta, F. Ogliaro, M. J. Bearpark, J. J. Heyd, E. N. Brothers, K. N. Kudin, V. N. Staroverov, T. A. Keith, R. Kobayashi, J. Normand, K. Raghavachari, A. P. Rendell, J. C. Burant, S. S. Iyengar, J. Tomasi, M. Cossi, J. M. Millam, M. Klene, C. Adamo, R. Cammi, J. W. Ochterski, R. L. Martin, K. Morokuma, O. Farkas, J. B. Foresman, D. J. Fox, Gaussian 16, Revision C.01, Gaussian, Inc., Wallingford CT,. (2016).

[14] RA. Friesner, RB. Murphy, MP. Repasky, LL. Frye, JR. Greenwood, TA. Halgren, PC. Sanschagrin, DT. Mainz Extra precision glide: Docking and scoring incorporating a model of hydrophobic enclosure for protein-ligand complexes. J. Med. Chem. 49 (2006) 6177–6196.

[15] Schrödinger Release 2021-4: LigPrep, Schrödinger, LLC, New York, NY,. (2021).

[16] Schrödinger Release 2021-4: FEP+, Schrödinger, LLC, New York, NY,. (2021).

[17] Schrödinger Release 2021-4: Protein Preparation Wizard; Epik, Impact, Schrödinger, LLC, New York, NY; Prime, , Schrödinger, LLC, New York, NY,. (2021).

[18] M. C. Romeu, P. T. C. Freire, A. P. Ayala, C. H. B. Antonio, L. S. Olivera, P. N. Bandeira, H. S. dos Santos, A. M. R. Teixeira, D. L. M. Vasconcelos, Synthesis, crystal structure, ATR-FTIR, FT-Raman and UV spectra, structural and spectroscopic

analysis of (3E)-4-[4-(dimethylamine)phenyl]but-3-en-2-one. Journal of Molecular Structure 1264 (2022) 133222.

[19] X. Wang, Y. Cheng, L. Wang, R. Wang, M. Zhang, Y. Yuan, J. Hu, W. Wang, Synthesis, crystal structure and negative hyperconjugation study of quinoxaline derivatives containing piperazine. Journal of the Indian Chemical Society 99 (2022) 100453.

[20] M. Singh, S. Anthal, P.J. Srijana, B. Narayana, B.K. Sarojini, U. Likhitha, Kamal, R. Kant, Novel supramolecular co-crystal of 3-aminobenzoic acid with 4-acetyl-pyridine: Synthesis, X-ray structure, DFT and Hirshfeld surface analysis. Journal of Molecular Structure 1262 (2022) 133061.

[21] P. Patil, S. Zangade, Synthesis, spectral characterization, single crystal X-ray diffraction, and antimicrobial properties of 1-(4-iodo-1-hydroxynaphthalen-2-yl)ethan-1-one. Chemical Data Collections 38 (2022) 100844.

[22] B. Zou, J. Xue, Y. Zhao, X. Zheng, Effect of the weak intermolecular C-H•••O=C hydrogen bonding, solvent polarity and concentration on the frequency of the C=O stretch mode of 2-thiophenecarboxaldehyde. Spectrochimica Acta Part A: Molecular and Biomolecular Spectroscopy 255 (2021) 119651.

[23] P. Kolandaivel, S. Rajendran, V. Nasif, S. Jayapalan, Synthesis, In Vitro Cytotoxicity, and DFT Studies of Novel 2-Amino Substituted Benzonaphthyridines as PDK1 Inhibitors. ChemistrySelect 7(2022) e202200288.

[24] D. Teffahi, S. Hocine, C.J. Li, Synthesis of Oxazolidinones, Dioxazolidinone and Polyoxazolidinone (A New Polyurethane) Via A Multi Component-Coupling of Aldehyde, Diamine Dihydrochloride, Terminal Alkyne and CO2. Letters in Organic Chemistry 9 (2012) 585-593.